



Structure-function relationship study for sulfated protein therapeutics using hydrophobic interaction chromatography and mass spectrometry

Hao Luo^{*}, David Mahon, Patrick Wong, Nandakumar Madayiputhiya, Yingchen Chen, Tara Stauffer, Li Tao, Ming Zeng

Biologics Development, Global Product Development and Supply, Bristol Myers Squibb, NJ, USA

ARTICLE INFO

Keywords:

Protein tyrosine sulfation
Hydrophobic interaction chromatography
Structure-function relationship
Mass Spectrometry

ABSTRACT

Protein tyrosine sulfation is a post-translational modification (PTM) that is rarely reported in recombinant therapeutic proteins. However, when sulfation does occur, the additional negative charge from the modification can influence intermolecular interactions and antigen-binding activity, making it a critical quality attribute that necessitates stringent control. In this study, we developed a unique hydrophobic interaction chromatography (HIC) method for the separation and quantification of a therapeutic bispecific antibody with varying degrees of sulfation. Despite the increased surface hydrophilicity of sulfated species, the HIC method provides enhanced retention. Baseline resolution was attained based on the degree of sulfation, independent of other PTMs such as C-terminal amidation and forced deamidation. Further structure-function relationship studies of enriched sulfated bispecific antibody species were conducted using mass spectrometry and fluorescence-linked immunosorbent assay (FLISA). These studies revealed that the tyrosine sulfation modification, which occurs in the complementarity-determining region (CDR), is a critical quality attribute and can adversely impact the antibody's binding to its cognate antigen. The evaluation of sulfation assay using HIC method confirmed it is an effective means for controlling this critical quality attribute.

1. Introduction

Protein tyrosine sulfation (PTS) is a post-translational modification (PTM) catalyzed by cellular enzymes. In this PTM, sulfate ion transported into the cytosol is first converted to a sulfo group donor substrate phosphoadenosine-5'-phosphosulfate (PAPS) under the catalysis of PAPS synthetase. Then PAPS is transported into Golgi, where its sulfo group is transferred to the side chain of tyrosine by tyrosylprotein sulfotransferase (TPST) 1 and 2, as shown in Fig. 1 [1,2].

PTS is a common PTM found on secretory and transmembrane proteins [3]. However, tyrosine sulfation on recombinant therapeutic proteins has been rarely reported. The first publication was from Zhao et al. [4], where sulfotyrosine was found on the light chain of an antibody produced in Chinese Hamster Ovary (CHO) cells. Tyrosine sulfation can affect protein-protein interactions and receptor-ligand binding [5]. Due to its potential impact on potency and immunogenicity, it is crucial to control tyrosine sulfation during the manufacturing process of therapeutic antibodies. Mitigation of tyrosine sulfation level by selecting CHO host cells with lower expression of sulfation pathway genes (e.g., TPST2

and PAPS transporter SLC35B2) and adding sodium chlorate in upstream process was reported [5]. In addition, structural modeling of tyrosine sulfation sites suggested that adjacent acidic amino acid residues and local secondary structure might play a role in making tyrosine a hot spot for sulfation [4,6,7]. Sulfinator, a software tool, was developed to predict tyrosine sulfation sites in protein sequences with an overall accuracy of 98 % [6,7]. In-silico identification of potential PTS site can also be used for molecular design and engineering at the early stage of biotherapeutic development [8]. Although PTS was not desired in many therapeutic proteins, a recent study of a broadly neutralizing monoclonal antibody (bNAb), CAP256V2LS, found that higher level of sulfation correlated to higher HIV-1 antigen binding activity [9]. A process preserving higher levels of PTS was designed and developed.

For therapeutic proteins, PTMs need to be extensively characterized due to their potential impact on drug's efficacy or safety properties [3,10–12]. Even if a PTM is not a critical quality attribute (CQA), its monitoring and control can still be required to ensure manufacturing consistency. Hence, developing robust and accurate analytical methods that are specific to certain PTM is necessary for biologics process

^{*} Corresponding author.

E-mail address: hao.luo@bms.com (H. Luo).

<https://doi.org/10.1016/j.jchromb.2023.123981>

Received 16 October 2023; Received in revised form 7 December 2023; Accepted 19 December 2023

Available online 22 December 2023

1570-0232/© 2023 Elsevier B.V. All rights reserved.

development and manufacturing control. To date, mass spectrometry (MS), ion exchange chromatography (IEX) and capillary electrophoresis (CE) are the most frequently used analytical techniques to determine PTMs' identity, location, and quantity [7,13–16][20]. However, due to the labile nature of the sulfo group, desulfation often occurs during mass spectrometric analysis, which converts sulfotyrosine back to tyrosine. It makes sulfation site identification and quantitation particularly challenging [4,7]. Although ion exchange chromatography is less susceptible to desulfation, its charge-based separation mode is not specific toward sulfation. Results from IEX are usually inflated by other PTMs that are usually more predominant, such as deamidation, glycation and etc.

Hydrophobic interaction chromatography (HIC) is a powerful technique for analyzing molecular variants in therapeutic proteins [17]. It is frequently used to separate and quantify tryptophan oxidation, aspartic acid isomerization, and succinimide formation. Additionally, HIC can be used to determine the drug-to-antibody ratio in antibody-drug conjugates (ADCs) [17,18]. Recently, a HIC method was reported for the separation and quantitation of tyrosine-O-sulfation proteoforms in monoclonal antibody CAP256V2LS [9]. Due to the introduction of a charged hydrophilic sulfo group, sulfated proteoforms are more hydrophilic and therefore eluted earlier than their native antibody in HIC [9].

In our study, we developed a unique HIC assay for tyrosine sulfation using Sepax Proteomix Butyl column. In this method, the retention increased with the sulfation degree, despite the reduced surface hydrophobicity. Additional assessment on sensitivity, linearity, and reproducibility indicates that this assay is suitable for quality control in the process development and manufacturing of biologics. Further structure–function relationship studies of the bispecific antibody revealed that the sulfation modification located in the CDR led to reduced binding to its cognate antigen.

2. Experimental

2.1. Materials and chemicals

The antibodies with PTS were manufactured at Bristol Myers Squibb. The sulfatase from abalone entrails, 8.0 M guanidine hydrochloride, sodium iodoacetate, ammonium sulfate, acetic acid, sodium acetate trihydrate, sodium phosphate monobasic monohydrate, sodium

phosphate dibasic and sodium chloride were purchased from Sigma-Aldrich (St. Louis, MO). CX-1 pH gradient buffer A pH 5.6 10× concentrate, CX-1 pH gradient buffer B pH 10.2 10× concentrate, trypsin, Asp-N endoproteinase, dithiothreitol (DTT), 0.5 M ethylenediaminetetraacetic Acid (EDTA) pH 8.0, trifluoroacetic acid, formic acid, 1 M tris(hydroxymethyl)aminomethane (Tris) pH 8.0, 1 M Tris pH 7.5, and acetonitrile were bought from Thermo scientific (Waltham, MA). methylcellulose, pI markers, SimpleSol protein solubilizer and fluorocarbon-coated cartridge were sourced from ProteinSimple (Santa Clara, CA), pharmalytes from Cytiva (Marlborough, MA), and Rapid PNGase F from New England Biolabs (Ipswich, MA).

2.2. Hydrophobic interaction chromatography (HIC)

2.2.1. Analytical scale

Analytical scale HIC analysis was performed on a Waters Alliance HPLC 2695 system. A Sepax Proteomix Butyl-NP5 column (4.6×100 mm, 5 μm particles, non-porous) or a Tosoh TSKgel Butyl-NPR column (2.5 μm particles, 4.6×100 mm) was used. A flow rate of 0.5 or 1 mL/min, a column temperature of 25 °C, and UV detection at 220 nm were applied throughout the HPLC runs. Mobile phase A (MPA) and mobile phase B (MPB) with different pHs and salt concentrations, and various gradient profiles were used during the method development. The conditions of mobile phase and gradient were specified under each figure. In addition, during the method development, the injection volume varied based on the concentrations of the samples, the amount of sample injected ranged between 10 and 50 μg. For the finalized method condition of Figure S1 (B1-B3), the sample concentration is 10 mg/mL and the injection volume is 5 μL.

2.2.2. Semi-preparative scale

Semi-preparative scale HIC fractionation was completed on an Agilent 1260 system with a G1364C fraction collector. A Sepax Proteomix Butyl-NP5 column (10×150 mm, 5 μm particles, non-porous) at room temperature was used with a flow rate of 4 mL/min and UV detection at 220 nm. Mobile phase A was 25 mM sodium acetate pH 4.0 with 2 M ammonium sulfate and mobile phase B was 25 mM sodium acetate pH 4.0. A linear gradient from 65 % mobile phase B to 100 % mobile phase B in 20 mins was used to separate the main peak and the two sulfated species. The column was equilibrated with initial mobile phase

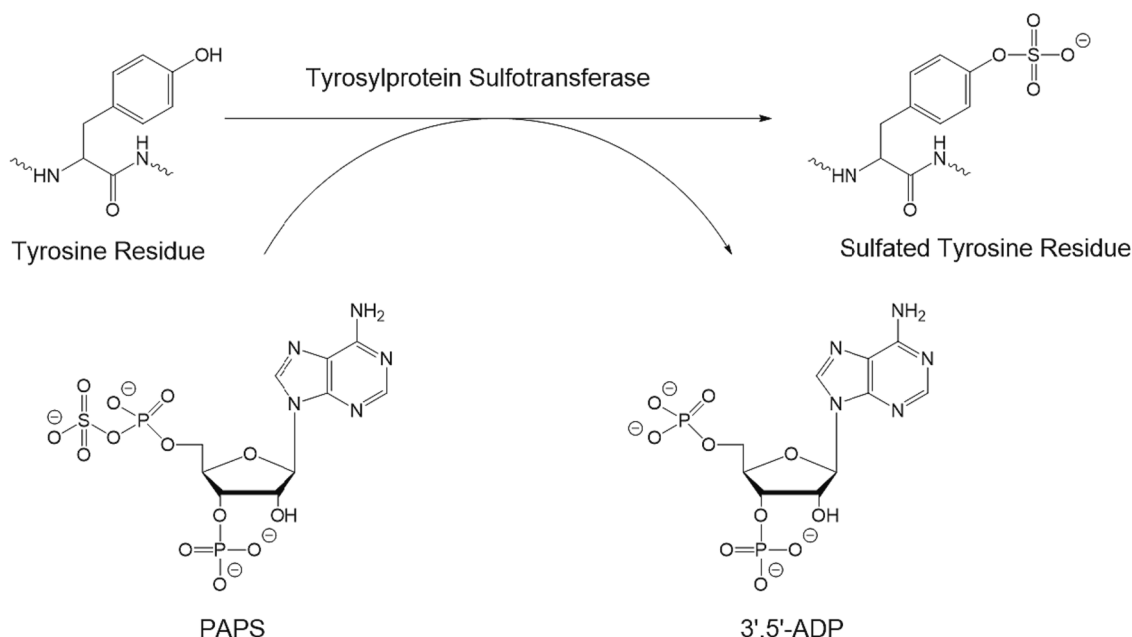


Fig. 1. Protein tyrosine sulfation.

composition for at least 5 mins prior to each injection. For each fractionation run, a 50 μ L injection of protein at a concentration of 50 mg/mL was made.

2.3. Imaged capillary isoelectric focusing (iCIEF)

iCIEF was performed on a ProteinSimple iCE3 instrument with Alcott 720NV Autosampler. Each sample was diluted to 2.5 mg/mL with ultrapure water (Milli-Q). The samples were then diluted to 1:10 (final concentration of 0.25 mg/mL) in a molecule-specific master mix consisting of 0.35 % methylcellulose, 4 % Pharmalytes (mixtures of 5–8 and 8–10.5), 20 % SimpleSol, and pI markers. The separation occurs in a Fluorocarbon-coated silica capillary (5 cm long with 100 μ m inner diameter), and the entire capillary is monitored in real time using a charge coupled device (CCD) camera imaging with absorbance at 280 nm. The injections were pre-focused at 1500 V for 1 min and focused at 3000 V for 12 min, respectively.

2.4. Ion exchange chromatography (IEX)

IEX analysis was conducted on a Waters Alliance HPLC 2695 system using a MabPac SCX-10 column (4 \times 250 mm, 5 μ m) at 25 $^{\circ}$ C. Mobile Phase A (MPA) was CX-1 buffer A (pH 5.6) and Mobile Phase B (MPB) was CX-1 buffer B (pH 10.2). A gradient profile of 0–30–55 % MPB at 0–1–30 min was applied for separation. The column was equilibrated with 100 % MPA for at least 5mins prior to each sample analysis. A flow rate of 0.4 mL/min and UV detection at 280 nm were used throughout the HPLC run. A 10 μ L injection of a sample at 1 mg/mL was made for each analysis.

2.5. Sulfatase treatment

Sulfotyrosine on the sulfated protein was converted back to tyrosine by sulfatase enzyme treatment. Sulfated protein solution was first exchanged into 0.1 M sodium acetate pH 5.0 with 0.1 M sodium chloride. Sulfatase was then added into the solution at a ratio of 1 unit/mg protein. The final protein and sulfatase concentrations were 1 mg/mL and 1 unit/mL respectively. The solution was incubated at 37 $^{\circ}$ C for 4–16 hrs.

2.6. Deamidation

Protein deamidation was conducted in 0.8 M Tris buffer at pH 9.0 with a protein concentration of 10 mg/mL. The solution was protected from light and kept at room temperature for 7 days.

2.7. Intact mass analysis

LC-MS based intact mass analysis was performed on a Waters Acquity I-Class UPLC[®] interfaced with a UV detector and a Waters Bio Accord Spectrometer. The analysis was carried out in deglycosylated non-reduced form. The target protein samples were initially deglycosylated using PNGaseF for 2 h at 37 $^{\circ}$ C. The deglycosylated protein samples were analyzed directly. The protein was chromatographically separated on a Waters (Milford, MA, USA) BEH 300 Å C4 column (2.1 \times 50 mm, 1.7 μ m particle size) at 50 $^{\circ}$ C set column temperature with a flow rate of 0.2 mL/min for a rapid 5-minute total run time. 10 μ L injection of sample at a concentration of 1 mg/mL was made. Mobile phase A was 0.1 % formic acid in water and mobile phase B was 0.1 % formic acid in acetonitrile. The intact protein was eluted at a total time between 2 and 3 min. Mass spectrometer was operated in an optimized condition to preserve tyrosine sulfation when analyzed in deglycosylated non-reduced form in positive ion mode. The spray temperature was set at 350 $^{\circ}$ C with a cone voltage of 150 V and capillary voltage of 1.5 kV. External calibration of the instrument was conducted prior to sample analysis. Data was acquired and analyzed using software UNIFI. Raw peak spectrum

deconvolution was conducted using the Maxent function of UNIFI software with a resolution setting of 25000. The relative quantification of mono- and di-sulfation peaks was conducted based on the relative peak intensity of the unmodified with that of mono-sulfation (+80 Da) and disulfation (+160 Da) peak intensity measured using the UNIFI Software.

2.8. Peptide mapping

About 200 μ g of protein was denatured and reduced with 6 M Guanidine Hydrochloride, 15 mM DTT, 5 mM EDTA in 100 mM Tris buffer (pH 8.0) at 37 $^{\circ}$ C for 20 min. Sample was alkylated with 40 mM Sodium Iodoacetate (Na-IAA) in the dark for 20 min. Following alkylation, samples were buffer exchanged into 50 mM Tris buffer (pH 7.5) using 10 K, micro dialysis cartridge. Final volume was adjusted to 200 μ L and incubated at 37 $^{\circ}$ C with 10 μ g of trypsin for 60 min, or with 4 μ g of Asp-N overnight. Digestion was quenched by lowering the sample pH with 3 μ L of 25 % trifluoroacetic acid. Typically, 7–10 μ g of digested samples was injected for peptide map analysis.

LC-MS peptide mapping was performed on a Waters Acquity I-Class UPLC[®] interfaced with a UV detector and a Thermo Scientific[™] Q Exactive[™] Plus Hybrid Quadrupole-Orbitrap[™] Mass Spectrometer. Peptides were separated on a Waters (Milford, MA, USA) BEH 300 Å C18 column (2.1 \times 150mm, 1.7 μ m particle) at 40 $^{\circ}$ C with a flow rate of 0.15 mL/min. Mobile phase A was 0.05 % trifluoroacetic acid in water and mobile phase B was 0.04 % trifluoroacetic acid in acetonitrile. Peptides were eluted with a gradient of 0–35 % B for 67 min, followed by 3 column wash steps of 30–80 % B for a total of 4 min. and 10 min. column equilibration. Mass spectrometer was operated in positive ion mode with MS resolution of 70,000 and MS/MS higher-energy C-trap dissociation (HCD) top 10 data dependent mode (DDA) with dynamic exclusion, scanning from 200 to 2000 m/z . External calibration of the instrument was conducted prior to sample analysis. Data was acquired using instrument vendor software Xcaliber and analyzed using Protein Metric INC software.

2.9. Binding characterization

The binding of the bispecific antibody to its target antigens was determined using a fluorescence-linked immunosorbent assay (FLISA). Native antibody or antibody spiked with different amounts of sulfated species were serially diluted and added to a 96-well plate coated with anti-human Fc antibody. Bound sample was detected by a cocktail containing antigen I with fluorescence I (Ex 405 nm/Em 650 nm) and antigen II with fluorescence II (Ex 565 nm/Em 615 nm). Following incubation of the fluorescent cocktail, plates were washed, and 200 μ L phosphate buffered saline (PBS) was added to each well. After that, both fluorescence values were measured simultaneously on a fluorescent plate reader. Dose response curves were generated by plotting fluorescent signal against antibody concentration ranges in Graphpad Prism (4-PL fit) and relative potency values were calculated against a reference standard.

3. Results and discussion

In this paper, we developed a method to separate and quantify tyrosine sulfation, focusing on a bispecific antibody that contains approximately 20–40 % of sulfotyrosine. This bispecific antibody is composed of three fragment antigen-binding (Fab) regions that bind to two different antigens simultaneously. Two of the Fabs bind to antigen I, while the remaining Fab binds to antigen II.

Through the use of peptide mapping combined with various MS/MS dissociation techniques and synthetic peptides, we determined that the sulfation site is located in the complementarity-determining region (CDR) of the Fab that binds to antigen I. Given that the antibody has two identical CDRs susceptible to sulfation, both mono-sulfated and disulfated species were expected and subsequently detected by intact

LC-MS. Although MS analysis has the capability to detect sulfation, it is not typically employed as a routine quality control technique. In addition, we observed desulfation during mass spectrometric analysis, and glycation (+162 Da) shared a close mass with di-sulfation (+160 Da).

An initial study on the effects of tyrosine sulfation during the drug discovery stage revealed a negative influence on the biological activity of the antibody [19]. This observation has led to a call for an accurate, specific, and robust quantitation method to effectively control sulfation.

3.1. Estimation of sulfated antibody by icIEF and IEX

Tyrosine sulfation introduces acidic sulfo groups to the antibody, prompting an exploration of imaged capillary isoelectric focusing (icIEF), a charge variants analysis technique that separates molecules based on their isoelectric point. Two antibody samples, produced from different cell lines, were analyzed and their charge profiles are depicted as black traces in Fig. 2. Both samples exhibited multiple acidic peaks, with sample 2 presenting a more complex profile with two additional basic peaks. These basic peaks, BP1 and BP2, were attributed to single and double C-terminal amidation respectively.

To identify the peaks associated with sulfation, the antibody was

treated with sulfatase to remove the sulfo group and then reanalyzed by icIEF. As shown by the red traces in Fig. 2, post-sulfatase treatment, the acidic group decreased while both the main and basic group increased. However, some acidic peaks remained, suggesting that sulfation variants overlapped with other acidic charge variants. As a result, the degree of sulfation could only be estimated by the change in the acidic group before and after sulfatase treatment. Using this approach, the degree of sulfation was estimated to be 27 % for sample 1 (Fig. 2A) and 12 % for sample 2 (Fig. 2B).

However, this method required two icIEF runs and a time-consuming enzyme treatment process for each sample, making it unsuitable for routine laboratory testing or for validation under good manufacturing practice (GMP) standards. More importantly, the degree of sulfation could be underestimated due to peak overlapping. For instance, some sulfated basic peaks could overlap with the main peak or be in the basic group region and move into a more basic region after sulfatase treatment. Similarly, some sulfated acidic peaks could move into adjacent less acidic peaks after sulfo group removal. In both cases, these sulfated species did not contribute to the overall decrease in the acidic group and were therefore not counted.

Ion exchange chromatography (IEX) with a pH gradient, another

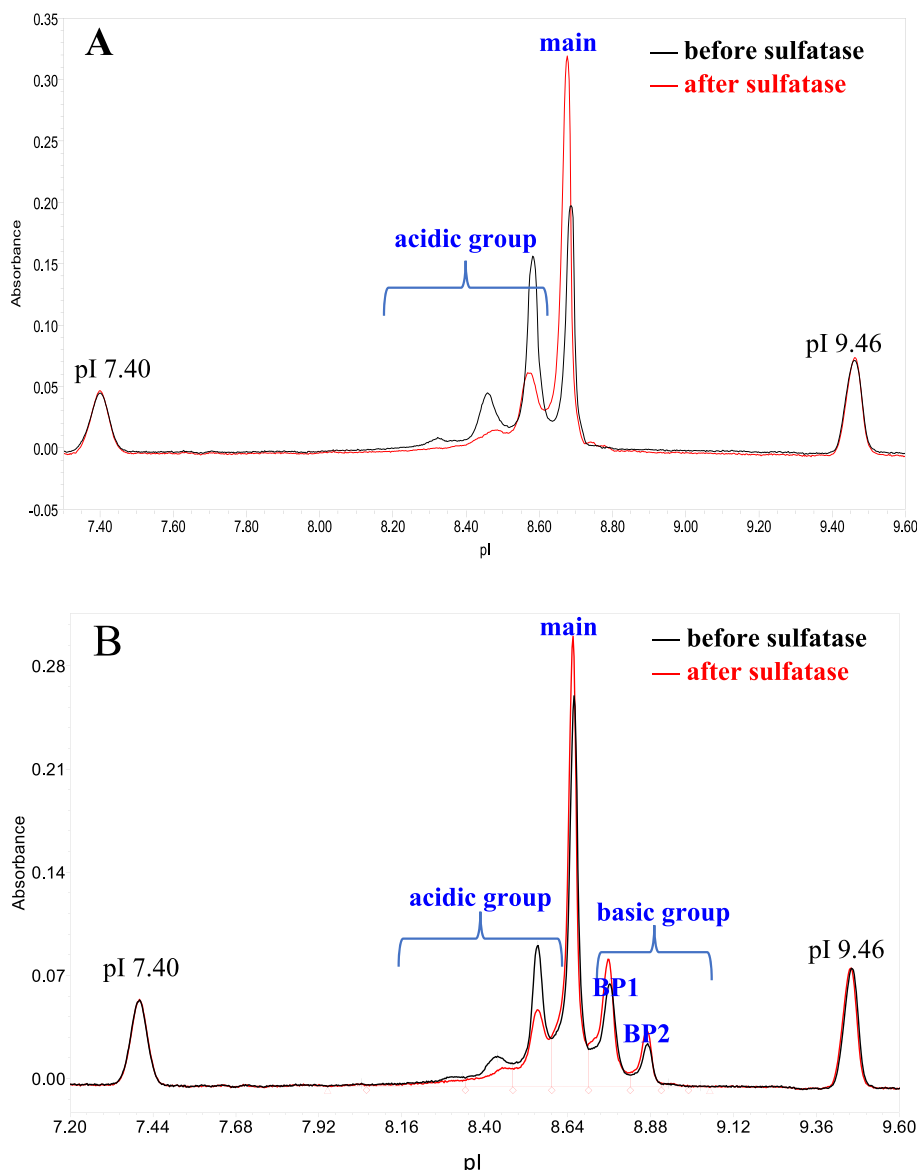


Fig. 2. icIEF of bispecific antibody before and after sulfatase treatment. A: Sample 1; B: Sample 2. icIEF conditions can be found in section 2.3.

commonly used charge variants analysis technique, was also tested. The charge variants profiles obtained from IEX before and after sulfatase treatment were similar to those obtained from icIEF, as shown in Fig. 3. Like icIEF, the IEX separation, which is based on charge, does not specifically target sulfation. Consequently, the level of sulfation can only be estimated by the decrease in the acidic group following the removal of the sulfo group. The degree of sulfation was estimated to be 28 % for sample 1 (Fig. 3A) and 20 % for sample 3 (Fig. 3B).

Upon examining the basic region of sample 3 (Fig. 3B), we noticed that there were three peaks: BP1, BP2, and s-BP2. s-BP2 is a small peak that elutes between BP1 and BP2. After sulfatase treatment, s-BP2 disappeared and an increase in the size of the adjacent more basic BP2 peak was observed. The concurrent change suggested that s-BP2 is the sulfated form of BP2.

As demonstrated in this case, some sulfated species like s-BP2 were not included in the decrease of the acidic group. Consequently, while charge separation methods like icIEF and IEX can detect the presence of tyrosine sulfation when combined with sulfatase treatment, they are not suitable for quantifying sulfation. This is due to limitations arising from peak overlapping and potential underestimation.

3.2. HIC method development for the quantification of sulfated antibody

Theoretically, sulfation alters not only the charge profiles of the antibody but also its surface hydrophobicity. While the impact of sulfation on the charge profile is indistinguishable from that of other PTMs such as deamidation, its impact on molecule hydrophobicity could be

specific due to the large and highly polarized sulfo group. Consequently, HIC, which separates proteins based on differences in their surface hydrophobicity, could be employed to develop a specific assay for sulfation.

Recently, HIC has been successfully used to enrich and quantify sulfated broadly neutralizing antibodies for improved HIV-1 binding activity [9]. However, the ProPac HIC-10 column used for sulfation assay in the publication was unable to resolve the sulfated species in our bispecific antibody.

Separation of sulfated bispecific antibody was observed on Butyl HIC columns, which have a different surface chemistry. Fig. 4 shows the separation on TSKgel Butyl-NPR column and Sepax Proteomix HIC butyl column using a typical HIC mobile phase at pH 7.0. Two minor peaks were separated from the main peak with completely opposite elution order on the two butyl HIC columns. After treatment with sulfatase, both minor peaks disappeared and the main peak increased. This confirmed that the minor peaks were related to tyrosine-O-sulfation and they were named sY1 and sY2. The largest peak in HIC was named sY0 because it increased after the elimination of the sulfo group and should be free of sulfation.

The identities of sY0, sY1 and sY2 were confirmed to be non-sulfated, mono-sulfated and di-sulfated species respectively in the following characterization (section 3.5). Due to their additional sulfo groups, sY1 and sY2 were expected to be more hydrophilic and elute earlier than sY0 as shown on TSKgel Butyl-NPR column. However, on Sepax Proteomix HIC butyl column, sY1 and sY2 eluted after sY0. This could be due to

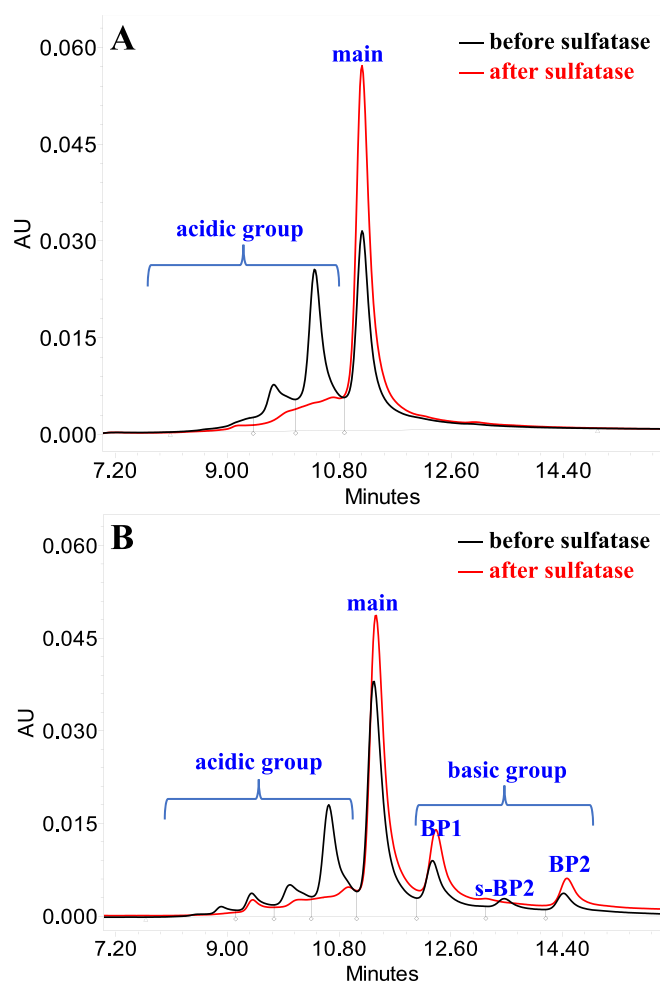


Fig. 3. IEX of bispecific antibody before and after sulfatase treatment. A: Sample 1; B: Sample 3, IEX conditions can be found in section 2.4.

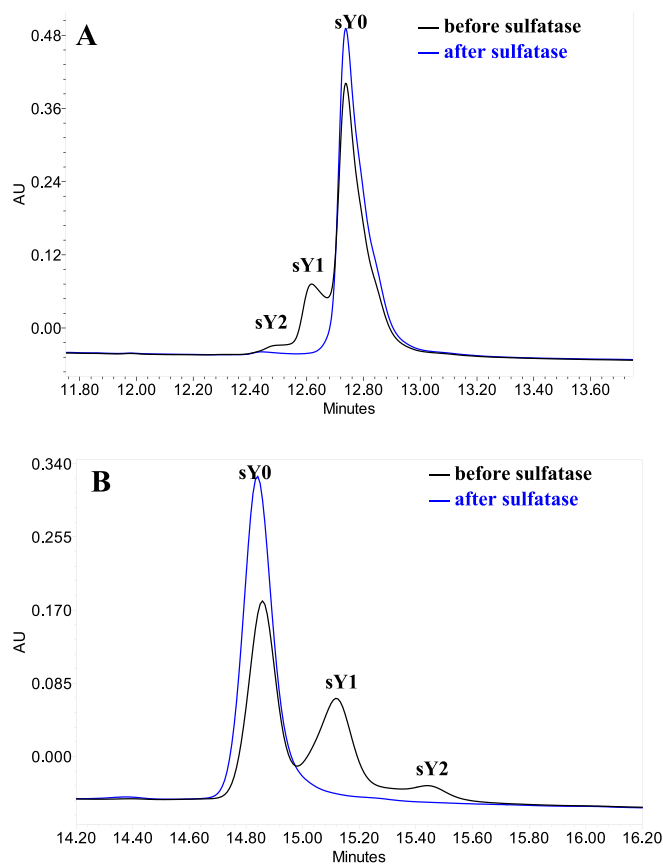


Fig. 4. HIC of bispecific antibody at pH 7 before and after sulfatase treatment. A: TSKgel Butyl-NPR column, 2.5 μ m particles, 4.6 \times 100mm; B: Sepax Proteomix HIC butyl-NP5 column, 5 μ m non-porous particles, 4.6 \times 100mm. The other HIC conditions were the same for A and B. column temperature: 25 $^{\circ}$ C; Flow rate: 1 mL/min; Detection: 220 nm; MPA: 80 mM sodium phosphate pH 7.0 with 2 M ammonium sulfate; MPB: 100 mM sodium phosphate pH 7.0; Gradient: 0–0–100–100 %MPB at 0–1–15–20 min; equilibrated the column with 100 %MPA for at least 5 min prior to each analysis.

some unique property of the stationary phase, such as mixed mode separation with HIC and anion exchange mechanism. Furthermore, a higher resolution was achieved using the Sepax column. For instance, the resolution between sY0 and sY1 is 1.0 on the Sepax column, compared to 0.6 on the TSKgel column.

The Sepax Proteomix HIC butyl column was selected for further method development due to its superior resolution. As depicted in Fig. 5, a shallower salt gradient resulted in further separation of sY1 and sY2 from sY0, but also led to peak broadening. Consequently, the resolution remained below 1.0, and baseline separation was not achieved.

To mitigate the potential impact of carboxylic groups on charge or hydrophobicity, mobile phases with pH values lower than 7 were tested. Fig. 6 illustrates that at lower pH values, sY1 and sY2 were better separated from sY0. A baseline resolution above 1.5 for all three peaks was achieved at pH 4.

To evaluate the performance of the newly developed HIC method at pH 4, bispecific antibody samples with varying degrees of sulfation were analyzed and the results were compared to those obtained using the icIEF or IEX methods described in section 3.1. The levels of mono-sulfated species was also determined by intact mass analysis after deglycosylation for comparison. Table 1 shows that the levels of mono-sulfated species sY1 from intact LC-MS were lower than those from HIC due to desulfation during MS analysis. The IEX and icIEF can only provide underestimated overall degrees of sulfation because of non-specific separation. Additionally, the two charge variants methods require an extra sulfatase treatment step, making them less robust, more variable and tedious.

3.3. HIC of sulfated antibodies with various degrees of amidation and deamidation

To further evaluate the specificity of the new HIC method, three samples with different charge profiles from cell line development were analyzed using both IEX and HIC. As shown in Figure S1 (A1-A3), sample 1 had the highest level of acidic group but no basic peaks. Sample 2 and 3 had fewer acidic variants but more basic peaks. As mentioned in section 3.1, there were three peaks in the basic group: BP1 and BP2 were singly and doubly amidated C-terminal species, respectively, while s-BP2 was sulfated BP2. Despite the significantly different charge profiles, all three samples demonstrated a consistent HIC separation pattern in Figure S1 (B1-B3) with only three major peaks: sY0, sY1 and sY2. This

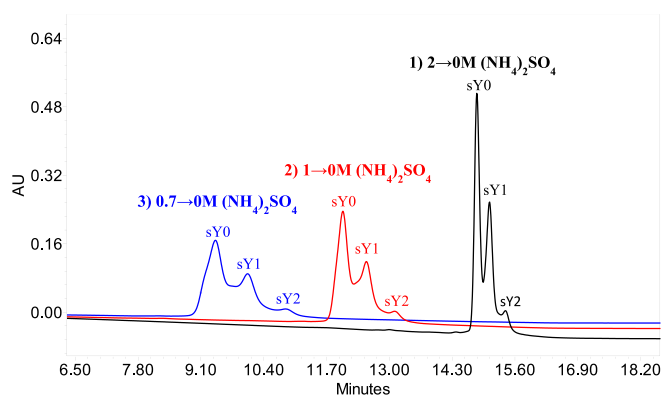


Fig. 5. HIC of bispecific antibody under different salt gradients at pH 7. HIC conditions: Sepax Proteomix HIC butyl-NP5 column, 5µm non-porous particles, 4.6×100mm at a column temperature of 25 °C; Flow rate: 1 mL/min; Detection: 220 nm; MPA: 80 mM sodium phosphate pH 7.0 with 2 M ammonium sulfate; MPB: 100 mM sodium phosphate pH 7.0; Gradient (1): 0–100–100 %MPB at 0–1–15–20 min; (2) 50–50–100–100 %MPB at 0–1–15–20 min; (3) 65–65–100–100 %MPB at 0–1–15–20 min; equilibrated the column with the initial mobile phase composition for at least 5 min prior to each analysis.

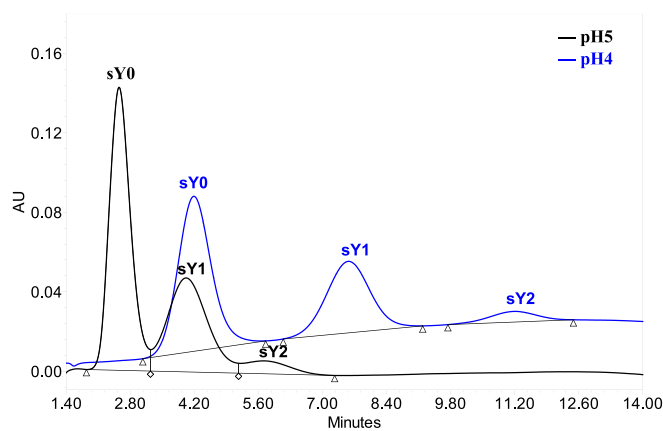


Fig. 6. HIC of bispecific antibody at low pHs. HIC conditions: Sepax Proteomix HIC butyl-NP5 column, 5µm non-porous particles, 4.6 × 100 mm at a column temperature of 25 °C; Flow rate: 1 mL/min; Detection: 220 nm; MPA: 25 mM sodium acetate pH 4.0 or 5.0 with 0.5 M ammonium sulfate; MPB: 25 mM sodium acetate pH 4.0 or 5.0; Gradient: 0–100–100 %MPB at 0–1–15–20 min; equilibrated the column with 100 %MPA for at least 5 min prior to each analysis.

Table 1

Results of sulfation assay using different methods for the bispecific antibody.

Method	sY1(%)	sY2(%)	total sulfation(%)		sY1(%) intact mass analysis
			IEX	icIEF	
Sample 1	36.3	5.1	28	27	28
Sample 2	22.4	2.1	NT	12	13
Sample 3	30.1	4.7	20	NT	15

NT: not tested.

suggested that the HIC method at pH 4 separates the bispecific antibody molecules primarily based on their degree of sulfation.

Forced deamidation, one of the most common degradation pathways that also affects the charge profile of proteins, was performed to assess whether the HIC method is influenced by this protein degradation. In the experiment, sample 2 was protected from light and treated under pH 9 at room temperature for 7 days. The deamidation caused an increase in the acidic group from 21.1 % to 36.3 %, as shown in Fig. 7A. Fig. 7B show that despite a significant shift in the charge profile towards the acidic region after the forced deamidation, the HIC profiles changed minimally. The sY0 peak experienced a slight decrease from 74.2 % to 73.4 %, accompanied by a corresponding increase in a small early eluting peak from 0.2 % to 0.9 %. The levels of sY1 and sY2 remained relatively stable at around 23.0 % and 2.7 %, respectively. These results further confirmed that the carboxyl group has no impact on sulfation determined by the HIC method for this bispecific antibody.

3.4. Isolation of antibodies with different amount of sulfation using HIC

To gain a more comprehensive understanding of the three peaks separated in HIC, they were isolated using a semi-preparative Sepax Proteomix butyl NP5 column at pH 4. The three fractions were collected, and buffer exchanged to the formulation condition of 20 mM histidine and 250 mM sucrose at pH 6.0.

The composition of the three fractions was first determined by analytical scale HIC, as shown in Figure S2. The sY0 fraction was clean, consisting of a single peak of sY0. The sY1 fraction contained approximately 10 % sY0 and 90 % sY1. The sY2 fraction comprised roughly 10 % of sY0, 10 % of sY1, 70 % of sY2, and another 10 % of an unknown minor peak that was non-detectable in the original antibody but was enriched together with sY2.

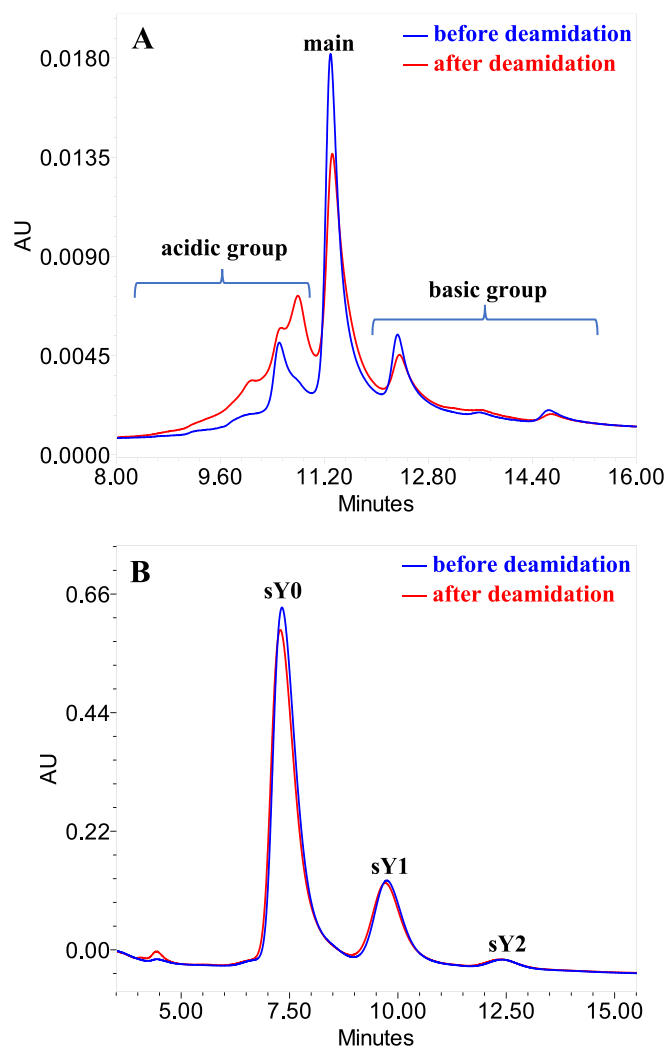


Fig. 7. IEX and HIC of bispecific antibody before and after deamidation. **A:** IEX of bispecific antibody before and after deamidation. IEX conditions are the same as Figure S1 (A1-A3). **B:** HIC of bispecific antibody before and after deamidation on Sepax Proteomix Butyl-NP5 at pH 4. HIC conditions are the same as Figure S1 (B1-B3).

3.5. Characterization of HIC fractions with different amount of sulfation

3.5.1. Intact mass analysis of HIC fractions

LC-MS based intact mass analysis was performed to characterize each HIC fraction. The analysis was carried out in deglycosylated non-reduced form, as described in section 2.7. The mass spectrum of the original antibody as a control, and the sY0, sY1 and sY2 fractions are shown in Figure S3. The mass of the main component in each fraction aligns with the structure of non-sulfated, mono-sulfated (+80 Da) and di-sulfated (+160 Da) antibody respectively. This confirms that the HIC fractions contain the target species with varying degrees of sulfation.

3.5.2. PTM analysis by peptide mapping for HIC fractions

PTM analysis by peptide mapping was performed for the original antibody as a control and the three HIC fractions. PTMs were identified by a shift in the retention time and/or mass-to-charge ratio (m/z) of the expected peptide. The exact location and nature of each PTM were identified by MS/MS. Various PTMs, including N- and C-terminal variants, Asn-deamidation, Asp isomerization, Met-oxidation, and Tyr-sulfation were observed. Asp-N endopeptidase digestion was used to obtain a unique fingerprint fragment for Tyr-sulfation measurement. All other PTMs were determined with trypsin digestion.

The levels of modification were quantified by peak area integration of the extracted ion chromatograms. The results for PTM were expressed as the percentage of total peak area for modified peptides. Considering the labile nature of sulfo group, sulfation levels were also measured by the percentage peak area of sulfated peptide fragments in the UV chromatogram at 214 nm. The PTM analysis results are summarized in Table 2. Due to the desulfation during mass spectrometric analysis, the sulfation levels from extracted ion chromatograms were considerably lower than the levels from UV chromatograms at 214 nm. Therefore, the latter was deemed to be more accurate and used in further discussion.

The sulfation levels were determined to be 1 %, 56 % and 81 % in the sY0, sY1 and sY2 fractions respectively. The results of sY0 and sY1 fractions were close to the theoretical values of 0 % and 50 % for pure non-sulfated and mono-sulfated antibodies. The sulfation level should be 100 % for pure di-sulfated antibody, and it was found to be 81 % in sY2 fraction. The slightly lower sulfation value can be attributed to the presence of approximately 10 % of non-sulfated and 10 % of mono-sulfated species in the sY2 fraction.

In addition, except for tyrosine sulfation, the levels of all other PTMs were similar between control and the three HIC fractions. Peptide mapping data further confirmed that the HIC separation for the bispecific antibody in this study is predominantly sulfation based with very limited interference from other PTMs.

3.5.3. Impact of sulfotyrosine on binding of bispecific antibody

In this study, the bispecific antibody is characterized by three Fab regions. Among these, two identical Fabs have an affinity for antigen I, while the remaining Fab region is designed to bind to antigen II. Tyrosine sulfation was identified in the CDR of the Fab that binds to antigen I.

To evaluate the impact of mono-sulfation and di-sulfation on binding to the two target antigens, sY1 and sY2 fractions were individually recombined with sY0 fraction at different ratios. This process generated discrete spiked samples containing various amounts of mono-sulfated or di-sulfated species. A fluorescent immunoassay that detects both binding events was employed in a single-assay format, where a discrete fluorescent signal reports each binding event.

The impact of the two sulfation species on the potency toward the two antigens was plotted against the proportion of sulfotyrosine in Fig. 8, and correlations were calculated. As shown in Fig. 8A, a modest reduction in binding to antigen I was observed with mono-sulfated species (sY1), where the potency decreased at a rate of 3.1 % for every 10 % increase in sY1. A larger reduction was observed when the CDR in both antigen I binding Fabs contained sulfotyrosine (sY2). The potency dropped at an accelerated rate of 7.5 % for each 10 % increase in sY2. As a result, tyrosine sulfation modification is considered a critical quality attribute that requires rigorous control to ensure binding toward antigen I.

On the other hand, as depicted in Fig. 8B, the potency toward antigen II remained relatively unchanged despite various amounts of

Table 2

Percentage of identified PTM in control and three HIC fractions.

PTM	Control	sY0 Fraction	sY1 Fraction	sY2 Fraction
Glu cyclization	0.8	0.8	1	1
Amidation	24.1	23.6	27.2	28.9
Oxidation 1	0.8	0.9	0.8	0.9
Oxidation 2	0.3	0.2	0.4	0.3
Oxidation 3	0.9	0.8	0.9	0.9
Oxidation 4	2.9	2.9	3.1	3.7
Oxidation 5	1.3	1.3	1.3	1.3
Oxidation 6	1.4	1.4	1.4	1.8
Deamidation 1	1.3	1.4	1.4	1.0
Deamidation 2	1.6	2.2	1.7	1.4
Isomerization	22.2	20.6	19.7	20.5
Sulfation ^{1,2}	16	1	56	81

¹ Data from Asp-N endopeptidase digestion

² Percentage peak area determined at 214 nm.

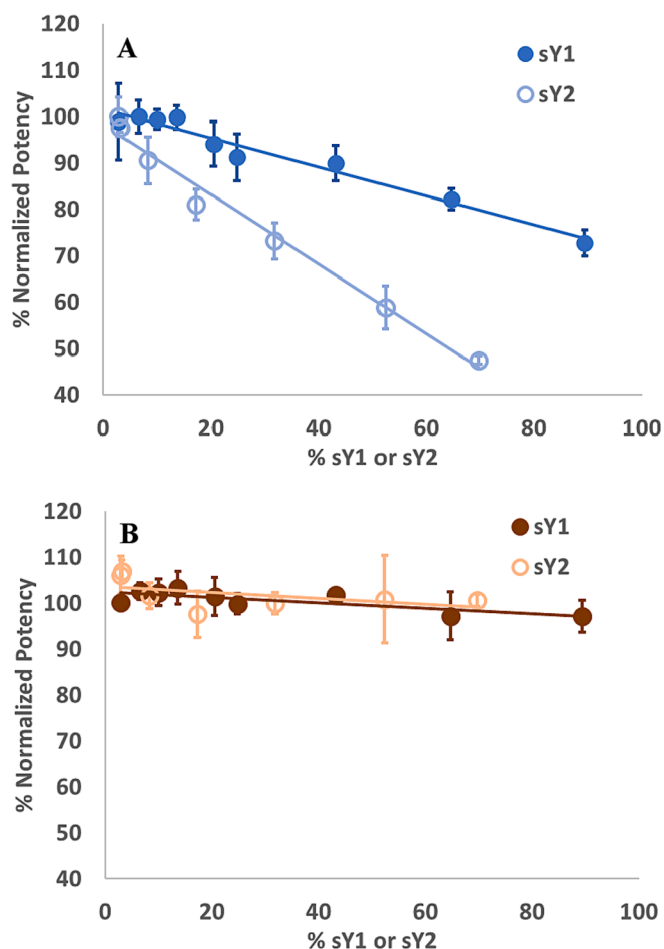


Fig. 8. Impact of tyrosine sulfation on antigen binding. A: correlation between percentage potency toward target antigen I and the composition of mono-sulfated (sY1) and di-sulfated (sY2) species. B: correlation between percentage potency toward target antigen II and the composition of mono-sulfated (sY1) and di-sulfated (sY2) species.

sulfotyrosine in the adjacent binding domain. The data indicates that sulfotyrosine substitution in the CDR of antigen I can adversely impact its binding to the corresponding antigen; the potency of the neighboring binding domain remains minimally affected.

3.6. Evaluation of HIC method for the quantitation of sulfated bispecific antibody

The HIC method was assessed for various parameters including specificity, sensitivity, precision, linearity, and accuracy for quantifying sY0, sY1, and sY2 of the bispecific antibody. Baseline separation was achieved with a resolution of 2.0 between sY0 and sY1, and 1.9 between sY1 and sY2 (as shown in Fig. 7). The limit of quantitation (LOQ) was determined to be 6 $\mu\text{g}/\text{mL}$ (30 ng) with a single-to-noise ratio of 11 using the broadest peak sY2. All three peaks demonstrated adequate precision in six replicate sample preparations with percent standard deviation (% RSD) less than 1 % for area percent and less than 5 % for peak area. Linearity evaluation was performed in a range of 50–150 % of the nominal concentration. sY0, sY1, and sY2 demonstrated good linearity with squared linear correlation coefficients of 0.9994, 0.9994 and 0.9993 respectively (Figure S4). The accuracy of the HIC method was assessed by evaluating the recoveries of sY0, sY1 and sY2 in the two series of solutions made for potency titration in section 3.5.3. The results indicated that recoveries ranged between 90 and 115 % across a broad spectrum of compositions, extending from a 100 % sY0 fraction to either

a 100 % sY1 fraction or a 100 % sY2 fraction. In summary, the evaluation results confirmed that the HIC method is suitable for quantifying the sulfated bispecific antibody.

4. Conclusions

The assay of protein tyrosine sulfation, whether by MS or charge-based separation methods like icIEF and IEX, was found to be inaccurate and often led to an underestimation of the sulfation level. In MS analysis, desulfation occurs during ionization, and glycation interferes with the quantitation of di-sulfation. Although the presence of tyrosine sulfation can be detected in icIEF and IEX when combined with sulfatase treatment, quantitation is limited due to the underestimation caused by the overlap of sulfated modifications and other negatively charged variants, such as deamidation.

In this paper, we introduce a novel HIC method that employs a Sepax butyl column at pH 4 to quantify sulfated molecules for recombinant therapeutic antibodies. Despite their increased surface hydrophilicity, sulfated species are more retained in this unique HIC method, likely due to a potential secondary anion exchange mechanism. In addition, this method demonstrates high specificity toward tyrosine sulfation and remains unaffected by common PTMs such as C-terminal amidation and forced deamidation in the sulfation assay of the bispecific antibody.

Further structure–function relationship study of the bispecific antibody revealed that the sulfation modification, located in the CDR, leads to reduced binding to its cognate antigen. This stresses the need for stringent quality control on sulfation modification. Evaluations of specificity, linearity, precision, sensitivity, and accuracy indicate that the HIC sulfation assay is suitable for routine laboratory testing for quality control purposes.

CRediT authorship contribution statement

Hao Luo: Formal analysis, Methodology, Writing – original draft, Writing – review & editing, Data curation, Investigation, Project administration. **David Mahon:** Data curation, Formal analysis, Investigation, Writing – original draft, Writing – review & editing. **Patrick Wong:** Data curation, Formal analysis, Investigation, Writing – original draft, Writing – review & editing. **Nandakumar Madayiputhiya:** Data curation, Formal analysis, Investigation, Writing – original draft, Writing – review & editing. **Yingchen Chen:** Data curation, Formal analysis, Investigation. **Tara Stauffer:** Supervision. **Li Tao:** Conceptualization, Supervision, Writing – review & editing. **Ming Zeng:** Conceptualization, Supervision, Writing – review & editing.

Declaration of Competing Interest

The authors declare that they have no known competing financial interests or personal relationships that could have appeared to influence the work reported in this paper.

Data availability

Data will be made available on request.

Appendix A. Supplementary material

Supplementary data to this article can be found online at <https://doi.org/10.1016/j.jchromb.2023.123981>.

References

- [1] Y. Kanan, R.A. Hamilton, D.M. Sherry, M.R. Al-Ubaidi, Focus on molecules: sulfotyrosine, *Exp. Eye Res.* 105 (2012) 85–86.
- [2] Y.S. Yang, C.C. Wang, B.H. Chen, Y.H. Hou, K.S. Hung, Y.C. Mao, Tyrosine sulfation as a protein post-translational modification, *Molecules* 20 (2015) 2138–2164.

- [3] S. Ramazi, J. Zahiri, Post-translational modifications in proteins: resources, tools and prediction methods, Database-Oxford, DOI ARTN baab012. 10.1093/database/baab012(2021).
- [4] J. Zhao, J. Saunders, S.D. Schussler, S. Rios, F.K. Insaiddo, A.L. Fridman, H. Li, Y. H. Liu, Characterization of a novel modification of a CHO-produced mAb: Evidence for the presence of tyrosine sulfation, *MAbs* 9 (2017) 985–995.
- [5] R. Liu, Y. Zhang, A. Kumar, S. Huhn, L. Hullinger, Z. Du, Modulating tyrosine sulfation of recombinant antibodies in CHO cell culture by host selection and sodium chlorate supplementation, *Biotechnol. J.* 16 (2021) e2100142.
- [6] F. Monigatti, E. Gasteiger, A. Bairoch, E. Jung, The Sulfinator: predicting tyrosine sulfation sites in protein sequences, *Bioinformatics* 18 (2002) 769–770.
- [7] F. Monigatti, B. Hekking, H. Steen, Protein sulfation analysis—A primer, *Biochim. Biophys. Acta* 1764 (2006) 1904–1913.
- [8] O. Tyshchuk, C. Gstottner, D. Funk, S. Nicolardi, S. Frost, S. Klostermann, T. Becker, E. Jolkver, F. Schumacher, C.F. Koller, H.R. Volger, M. Wuhrer, P. Bulau, M. Molhoj, Characterization and prediction of positional 4-hydroxyproline and sulfotyrosine, two post-translational modifications that can occur at substantial levels in CHO cells-expressed biotherapeutics, *MAbs* 11 (2019) 1219–1232.
- [9] C.X. Cai, N.A. Doria-Rose, N.A. Schneck, V.B. Ivleva, B. Tippett, W.R. Shadrick, S. O'Connell, J.W. Cooper, Z. Schneiderman, B. Zhang, D.B. Gowetski, D. Blackstock, J. Demirji, B.C. Lin, J. Gorman, T. Liu, Y. Li, A.B. McDermott, P. D. Kwong, K. Carlton, J.G. Gall, Q.P. Lei, Tyrosine O-sulfation proteoforms affect HIV-1 monoclonal antibody potency, *Sci. Rep.* 12 (2022) 8433.
- [10] G. Walsh, R. Jefferis, Post-translational modifications in the context of therapeutic proteins, *Nat. Biotechnol.* 24 (2006) 1241–1252.
- [11] G. Walsh, Post-translational modifications of protein biopharmaceuticals, *Drug Discov. Today* 15 (2010) 773–780.
- [12] N. Jenkins, L. Murphy, R. Tyther, Post-translational modifications of recombinant proteins: significance for biopharmaceuticals, *Mol. Biotechnol.* 39 (2008) 113–118.
- [13] M. Mann, O.N. Jensen, Proteomic analysis of post-translational modifications, *Nat. Biotechnol.* 21 (2003) 255–261.
- [14] D. Virág, B. Dalmadi-Kiss, K. Vékey, L. Drahos, I. Klebovich, I. Antal, K. Ludányi, Current trends in the analysis of post-translational modifications, *Chromatographia* 83 (2020) 1–10.
- [15] S. Mohammed, A.J. Heck, Strong cation exchange (SCX) based analytical methods for the targeted analysis of protein post-translational modifications, *Curr. Opin. Biotechnol.* 22 (2011) 9–16.
- [16] A. Trappe, F. Füssl, S. Carillo, I. Zaborowska, P. Meleady, J. Bones, Rapid charge variant analysis of monoclonal antibodies to support lead candidate biopharmaceutical development, *J. Chromatogr. B* 1095 (2018) 166–176.
- [17] M. Haverick, S. Mengisen, M. Shameem, A. Ambrogelly, Separation of mAbs molecular variants by analytical hydrophobic interaction chromatography HPLC: overview and applications, *MAbs*, Taylor & Francis, 2014, pp. 852–858.
- [18] S. Fekete, J.-L. Veuthey, A. Beck, D. Guillarme, Hydrophobic interaction chromatography for the characterization of monoclonal antibodies and related products, *J. Pharm. Biomed. Anal.* 130 (2016) 3–18.
- [19] C.B. Lietz, E. Deyanova, Y. Cho, J. Cordia, S. Franc, S. Kabro, S. Wang, D. Mikolon, D.D. Banks, Identification of tyrosine sulfation in the variable region of a bispecific antibody and its effect on stability and biological activity, *MAbs*, 15, Taylor & Francis, 2023, p. 2259289.
- [20] K. Faserl, B. Sarg, P. Gruber, H.H. Lindner, Investigating capillary electrophoresis-mass spectrometry for the analysis of common post-translational modifications, *Electrophoresis* 39 (2018) 1208–1215.